Self-Assembly of Nucleoamphiphiles: Investigating Nucleosides Effect and the Mechanism of Micrometric Helix Formation

Carole Aimé,[†] Sabine Manet,[†] Takao Satoh,[‡] Hirotaka Ihara,[‡] Keon-Young Park,[†] Frédéric Godde,[†] and Reiko Oda*,[†]

Institut Européen de Chimie et Biologie, UMR 5248 CBMN, CNRS-Université Bordeaux 1-ENITAB, IECB, 2 rue Robert Escarpit, 33607 Pessac, France, and Department of Applied Chemistry and Biochemistry, Kumamoto University, 2-39-1, Kurokami, Kumamoto 860-8555, Japan

Received July 13, 2007. In Final Form: August 30, 2007

A new family of self-assembling systems based on nucleoamphiphiles is described. Nano to micrometric left-handed helix formation in aqueous solution was induced simply by complexing a GMP or an AMP with a nonchiral monocationic amphiphile. The assembling behavior such as micellar formation, monolayer at air−water interface, as well as the aggregates in solution of these nucleoamphiphiles are strongly influenced by the presence of nucleosides in solution. The observed effects depend on the properties of complexed nucleotides and nucleosides with a complex mixture of π stacking, hydrophobicity of the bases, and hydrogen bonding.

Introduction

Self-assembly is the driving force for the formation of numerous nanostructures from a broad diversity of building blocks. Soft[1] and biological[2] materials have attracted much interest for their self-assembling properties. Indeed, self-assembly through biological materials such as proteins and nucleic acids is mostly governed by multiple weak interactions. DNA is a particularly good model in the attempt to induce self-association through weak interactions, as the stability of the DNA double helix results from multiple interactions of nucleobases via unspecific stacking interactions along with weak but specific hydrogen bonds (Watson−Crick configuration) between complementary bases: adenine and thymine/uracil; cytosine and guanine. Bio-inspired self-assembly systems have been designed with such building blocks to develop systems that mimic nature.[3] Molecular recognition, through specific hydrogen bonds, has been the subject of investigations to induce formation of macromolecular assemblies by molecular recognition. However, in water there is heavy competition between specific intermolecular interactions and nonspecific hydrogen bonds with water molecules.[4] To overcome this drawback and promote stabilization of structures, additional attractive interactions are required. The use of amphiphilic molecules provides an interesting way to stabilize the supramolecular structure via the hydrophobic effect. Indeed, the hydrophobic effect is the driving force for micelle and membrane formation, characteristic of surfactant self-assembly. Nucleoamphiphile systems have been developed in this context to take advantage of the recognition properties[5] as well as the self-assembling properties[6] at the air−water interface,[7] water−solid interface,[8] or Langmuir−Blodgett films.[9] The surface force apparatus[10] and mass spectrometry[8,11] have also been used to measure the interaction between aggregates of nucleolipids. Studies on the interaction between supramolecular aggregates such as vesicles or micelles with nucleolipids have also been reported.[5,12] These aggregates can provide the appropriate environment for internucleobase recognition, and the molecular organization can be perturbed by locally inducing variations in spectroscopic signals.

While the systems studied so far involve covalent interactions between both elements, we have developed a new system where the nucleotides and the amphiphiles are complexed by electrostatic interactions.[13] The approach presented herein involves a monocationic surfactant having two hydrophobic chains of 12 and 14 carbons (C_{12} and C_{14}) complexed with monoanionic guanosine 5′-monophosphate (GMP) and adenosine 5′-monophosphate (AMP), respectively (Scheme 1). The systems will be noted

* r.oda@iecb.u-bordeaux.fr.
† CNRS-Université Bordeaux.
‡ Kumamoto University.

(1) Hamley, I. W. *Angew. Chem., Int. Ed.* **2003**, *42*, 1692.
(2) (a) Lowe, C. R. *Curr. Opin. Struct. Biol.* **2000**, *10*, 428. (b) Niemeyer, C. M. *Angew. Chem., Int. Ed.* **2001**, *40*, 4128.
(3) (a) Seeman, N. C. *Nature (London)* **2003**, *421*, 427. (b) Ding, B.; Sha, R.; Seeman, N. C. *J. Am. Chem. Soc.* **2004**, *126*, 10230. (c) Liao, S.; Seeman, N. C. *Science* **2004**, *306*, 2072. (d) Matsuura, K.; Yamashita, T.; Igami, Y.; Kimizuka, N. *Chem. Commun.* **2003**, 376. (e) Kim, K.; Masumoto, K.; Matsuura, K.; Kimizuka, N. *Chem. Lett.* **2006**, *35*, 486.
(4) Saenger, W. *Principles of Nucleic Acid Structure*; Springer-Verlag: New York, 1984.
(5) (a) Onda, M.; Yoshihara, K.; Koyano, H.; Ariga, K.; Kunitake, T. *J. Am. Chem. Soc.* **1996**, *118*, 8524. (b) Berti, D.; Baglioni, P.; Bonaccio, S.; Barsacchi-Bo, G.; Luisi, P. L. *J. Phys. Chem. B* **1998**, *102*, 303. (c) Berti, D.; Luisi, P. L.; Baglioni, P. *Colloids Surf., A: Physicochem. Eng. Aspects* **2000**, *167*, 95. (d) Baglioni, P.; Berti, D. *Curr. Opin. Colloid Interface Sci.* **2003**, *8*, 55. (e) Shimizu, T.; Iwaura, R.; Masuda, M.; Hanada, T.; Yase, K. *J. Am. Chem. Soc.* **2001**, *123*, 5947. (f) Iwaura, R.; Yoshida, K.; Masuda, M.; Yase, K.; Shimizu, T. *Chem. Mater.* **2002**, *14*, 3047. (g) Iwaura, R.; Yoshida, K.; Masuda, M.; Ohnishi-Kameyama, M.; Yoshida, M.; Shimizu, T. *Angew. Chem., Int. Ed.* **2003**, *42*, 1009. (h) Iwaura, R.; Hoeben, F. J. M.; Masuda, M.; Schenning, A. P. H. J.; Meijer, E. W.; Shimizu, T. *J. Am. Chem. Soc.* **2006**, *128*, 13298.
(6) (a) Haruta, O.; Nishida, J.; Ijiro, K. *Colloids Surf., A: Physicochem. Eng. Aspects* **2006**, *284−285*, 326. (b) Moreau, L.; Barthelemy, P.; El Maataoui, M.; Grinstaff, M. W. *J. Am. Chem. Soc.* **2004**, *126*, 7533. (c) Moreau, L.; Ziarelli, F.; Grinstaff, M. W.; Barthelemy, P. *Chem. Commun.* **2006**, 1661. (d) Fortini, M.; Berti, D.; Baglioni, P.; Ninham, B. W. *Curr. Opin. Colloid Interface Sci.* **2004**, *9*, 168. (e) Bombelli, F. B.; Berti, D.; Almgren, M.; Karlsson, G.; Baglioni, P. *J. Phys. Chem. B* **2006**, *110*, 17627. (f) Park, S. M.; Lee, Y. S.; Kim, B. H. *Chem. Commun.* **2003**, 2912. (g) Sugiyasu, K.; Numata, M.; Fujita, N.; Park, S. M.; Yun, Y. J.; Kim, B. H.; Shinkai, S. *Chem. Commun.* **2004**, 1996.
(7) (a) Shimomura, M.; Nakamura, F.; Ijiro, K.; Taketsuna, H.; Tanaka, M.; Nakamura, H.; Hasebe, K. *J. Am. Chem. Soc.* **1997**, *119*, 2341. (b) Berti, D.; Franchi, L.; Baglioni, P. *Langmuir* **1997**, *13*, 3438.
(8) Weisser, M.; Käshammer, J.; Menges, B.; Matsumoto, J.; Nakamura, F.; Ijiro, K.; Shimomura, M.; Mittler, S. *J. Am. Chem. Soc.* **2000**, *122*, 87.
(9) Li, C.; Huang, J.; Liang, Y. *Langmuir* **2000**, *16*, 7701.
(10) Pincet, F.; Perez, E.; Bryant, G.; Lebeau, L.; Mioskowski, C. *Mod. Phys. Lett. B* **1996**, *10*, 81.
(11) Iwaura, R.; Ohnishi-Kaneyama, M.; Yoshida, M.; Shimizu, T. *Chem. Commun.* **2002**, 2658.
(12) Iwaura, R.; Yoshida, K.; Masuda, M.; Ohnishi-Kameyama, M.; Yoshida, M.; Shimizu, T. *Angew. Chem., Int. Ed.* **2003**, *42*, 1009.
(13) Wang, Y.; Desbat, B.; Manet, S.; Aimé, C.; Labrot, T.; Oda, R. *J. Colloid Interface Sci.* **2005**, *283* (2), 555.

10.1021/la702105s CCC: $37.00
Published on Web 11/10/2007 PAGE EST: 10.1

Scheme 1. Structures of the Nucleoamphiphiles Studied[a]

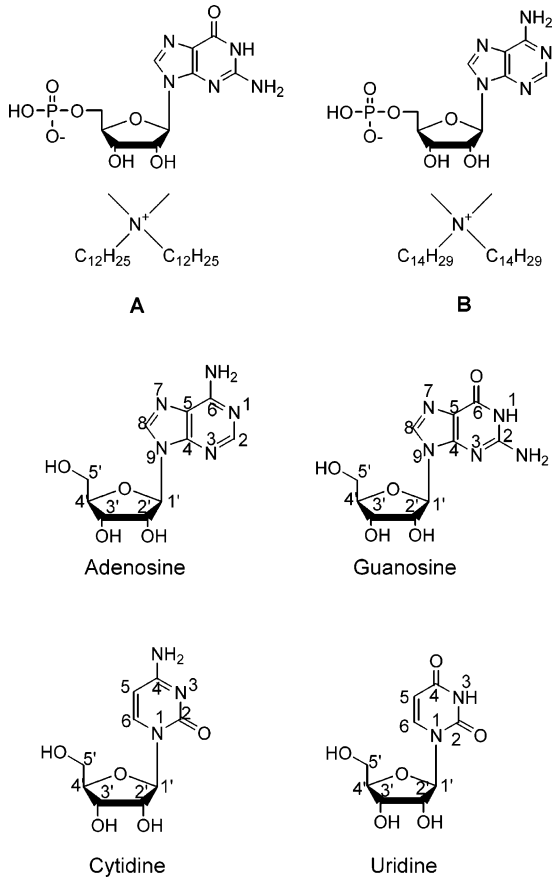

[a] (A) C_{12}GMP surfactant. C_{12} monocationic amphiphile molecule complexed with guanosine 5′-monophosphate (GMP). (B) C_{14}AMP surfactant. C_{14} monocationic amphiphile molecule complexed with adenosine 5′-monophosphate (AMP), and structures of the four non ionic nucleosides added in the experiments presented herein: guanosine (G), adenosine (A), cytidine (C), and uridine (U). The numbers indicate the proton positions for NMR analysis.

hereafter as C_{12}GMP (Scheme 1A) and C_{14}AMP (Scheme 1B). We investigated the role of the nucleotide (nucleobase−ribose−phosphate) complexed (GMP vs AMP) with the amphiphilic molecules and the role of additional non-ionic nucleosides (nucleobase−ribose): adenosine (A), cytidine (C), guanosine (G), and uridine (U) (Scheme 1). C_{12}GMP and C_{14}AMP aggregation behaviors were systematically investigated in the presence of each nucleoside. The assembling behaviors of these systems were studied both at molecular and supramolecular levels, by means of critical aggregation concentration (cac) measurements, Langmuir isotherms, and optical and electron microscopies. We show that the interactions between the nucleotides (counterions) and nucleosides control aggregation states of the nucleo-amphiphiles and the morphologies of their self-assemblies.

Surprisingly, these surfactants self-assembled in water into micrometric chiral helical structures. As we have previously reported that nonchiral dicationic gemini surfactants could self-assemble into chiral fibers in the presence of chiral tartrate counterions[14] or when complexed with oligo-alanine peptides,[15] this represents a new example of chirality transfer: the chirality of the sugar moiety of the nucleotide is expressed at the supramolecular level.

It was clearly observed that the interactions between ionic nucleoamphiphiles and non-ionic nucleosides are influenced by the nature of the different bases. Each nucleoside possesses numerous H-bond donors and acceptors, and bases are able to interact in multiple H-bond configurations when they are implied in self-assemblies. Along with higher hydrophobicity and $\pi-\pi$ stacking ability of purine bases (A and G) compared to pyrimidine bases (C and U), these factors influence the assembling behaviors of these nucleobases in a complex manner at both the molecular and supramolecular levels. Understanding the interactions among nucleotide-based amphiphilic molecules gives an original and precise view of the specific and nonspecific interactions, which is extremely important in an attempt to control and design new bioarchitectures.

Experimental Section

Materials. The nucleoamphiphiles are obtained via two ion exchanges in water. We start from the equivalent cationic surfactant (C_{12} or C_{14}) complexed with bromide counterion. The first ion exchange gives rise to the surfactant complexed with acetate and finally complexed with the desired nucleotide (GMP or AMP).

Synthesis of C_{12} and C_{14} Acetate. Cationic surfactants, dialkyldimethylammonium bromide (n = 12 and 14), were purchased from Fluka and used without any further purification. The surfactant was mixed with silver acetate (1 equiv) in methanol. The mixture is stirred for 30 min at 50 °C until the formation of a black precipitate of silver bromide. The acetate surfactant is soluble in methanol. Silver bromide is filtered on Celite to give a colorless solution. After evaporation, the product is dissolved in a mixture of chloroform/methanol (9/1) (v/v), precipitated with acetone, filtered, and dried under vacuum.

Synthesis of C_{12} and C_{14} Nucleotide. In the methanol solution of the acetate surfactant, the desired acidic nucleotide was added (1.1 equiv). After evaporation, the product is dissolved in a mixture of chloroform/methanol (9/1) (v/v), precipitated with acetone, filtered, and dried under vacuum. Guanosine 5′-monophosphate and adenosine 5′-monophosphate were purchased from Fluka and Acros Organics, respectively, and used without any further purification. ^{1}H (400 MHz) and ^{13}C (100 MHz) NMR spectra were recorded with a Bruker 400 Ultrashield spectrometer. Residual solvent peaks were used as internal standards. The following notation was used for the ^{1}H NMR splitting patterns: singlet (s), doublet (d), triplet (t), multiplet (m), and double doublet (dd).

C_{12}GMP. ^{1}H NMR (400 MHz, CD_3OD, 25 °C, δ ppm): 8.08 (1H, s); 5.85 (1H, d, ^3J = 6.36 Hz); 4.76 (1H, dd, ^3J = 5.14 Hz, ^3J = 6.36 Hz); 4.38 (1H, dd, ^3J = 2.45 Hz, ^3J = 5.14 Hz); 4.18 (1H, m); 4.14 (1H, m); 4.07 (1H, m); 3.28 (4H, m); 3.05 (6H, s); 1.74 (4H, m); 1.38 (4H, m); 1.29 (32H, m); 0.90 (6H, t, ^3J = 6.85 Hz). ^{13}C NMR (400 MHz, CD_3OD, 25 °C, δ ppm): 138.45; 89.25; 75.05; 72.36; 65.85; 65.22; 51.20; 49.64; 49.42; 49.21; 48.99; 48.79; 48.57; 48.36; 48.27; 48.11; 48.06; 47.98; 47.92; 47.88; 33.08; 30.75; 30.63; 30.52; 30.48; 30.20; 27.37; 23.74; 23.49; 14.43;

C_{14}AMP. ^{1}H NMR (400 MHz, CD_3OD, 25 °C, δ ppm): 8.56 (1H, s); 8.21 (1H, s); 6.09 (1H, d, ^3J = 6.11 Hz); 4.67 (1H, m); 4.41 (1H, dd, ^3J = 3.11 Hz, ^3J = 4.76 Hz); 4.24 (1H, m); 4.12 (2H, m); 3.28 (4H, m); 3.05 (6H, s); 1.73 (4H, m); 1.38 (4H, m); 1.29 (40H, m); 0.89 (6H, t, ^3J = 13.36 Hz). ^{13}C NMR (400 MHz, CD_3OD, 25 °C, δ ppm): 152.76; 141.46; 141.43; 123.10; 123.08; 121.08; 107.86; 88.89; 86.14; 86.10; 86.06; 76.35; 72.44; 65.96; 65.91; 65.86; 65.20; 51.21; 49.64; 49.42; 49.32; 49.21; 48.99; 48.79; 48.57; 48.36; 48.15; 48.08; 48.00; 47.95; 47.90; 47.84; 47.80; 47.76; 47.70; 47.64; 47.59; 33.09; 30.77; 30.63; 30.49; 30.18; 27.35; 25.62; 23.74; 23.48; 14.44.

Nucleoamphiphile samples in water exhibit pH values which depend on the surfactant concentrations. For C_{12}GMP, pH is around 4.5−5.5 at 0.4 mM (cmc measurement) and 3 at 20 mM, (morphology and NMR studies) and for C_{14}AMP, pH is around 5−6 at 0.4 mM (cmc measurement) and 4−5 at 10 mM (morphology and NMR

(14) (a) Oda, R.; Huc, I.; Candau, S. J. *Angew. Chem., Int. Ed.* **1998**, *37*, 2689. (b) Oda, R.; Huc, I.; Schmutz, M.; Candau, S. J.; MacKintosh, F. C. *Nature (London)* **1999**, *399*, 566. (c) Berthier, D.; Buffeteau, T.; Léger, J. M.; Oda, R.; Huc, I. *J. Am. Chem. Soc.* **2002**, *124*, 13486. (d) Brizard, A.; Aime, C.; Labrot, T.; Huc, I.; Berthier, D.; Artzner, F.; Desbat, B.; Oda, R. *J. Am. Chem. Soc.* **2007**, *129*, 3754.

(15) Brizard, A.; Kiagus Ahmad, R.; Oda, R. *Chem. Commun.* **2007**, 2275.

studies), respectively. The pH values in the presence of added nucleosides are summarized in the Supporting Information. At these pH, the adenosine and guanosine are both uncharged. No depurination reaction was observed over a month as controlled by NMR.[16]

Conductivity Measurements. The conductivity was measured with a Consort C830 (Belgium) conductimeter with an SK10T platinum electrode embedded in glass (cell constant 1.0 cm^{-1}). The measurements were performed in a temperature-controlled double-walled glass container with water circulation. For the critical aggregation concentration (cac) measurements, a stock solution of surfactant at a concentration about 10 times the expected cac was successively added to 4 mL of deionized water (Purelab Prima Elga, 18.2 MΩ cm) or to 4 mL of 2 mM nucleoside solution depending on the experiment. Sufficient time was given between additions (>1 min) until the conductivity reached equilibrium after each addition. The cac values were taken as the break in the conductivity curves.

Krafft Temperatures (T_k). The Krafft temperature is the minimum temperature at which the hydrated surfactant becomes soluble. Below T_k, a gel or precipitate is formed. T_k valus were also determined using the electrical conductivity method[17] (see Supporting Information) combined with visual observation. Since the conductivity is strongly influenced by the presence of any metastable or kinetically controlled aggregates, care was taken so that all samples were treated in the same manner. The powder of surfactant was first solubilized in water to obtain the solution of about 1% w/w, and then it was freeze-dried to get a very fine airy powder. This powder was again dispersed in water to obtain 3 mM solutions, much above the cmc of all the investigated surfactants. To make sure that all the samples formed well-hydrated precipitate, the solutions were plunged into liquid nitrogen to get fast precipitation without forming a gel and freezing, and then they were kept at 2 °C for several hours so that they melted. The solutions with precipitates were introduced into the conductivity cell, and the conductivity was measured as the temperature was increased between 2 and 80 °C with a temperature increase rate of 1 °C per 10 min. Hydrophobic chain length and counterion nature are two key parameters in determining T_k. The longer the chain length, the higher the T_k. Concerning the nature of the counterion, guanosine and derivatives are notoriously intractable in the laboratory. Guanosine is neither the most hydrophobic nucleoside[18] nor the most lipophilic one.[19] However, it is the most insoluble nucleoside in water, because it self-associates with its edges having self-complementary H-bond donors and acceptors, and with its polarizable aromatic surface with a strong molecular dipole, ideal for stacking.[20] In our systems, for a constant hydrophobic chain length, C_nGMP had higher T_k values than C_nAMP (n is the number of carbons), therefore less soluble. In order to get comparable systems having similar T_k values, we used shorter chain lengths for GMP than for AMP (C_{12} vs C_{14}) to compensate precipitation propensity. Indeed, T_k values measured for both systems (C_{12}GMP and C_{14}AMP at 3 mM) by conductivity measurements are around 35 °C (Supporting Information).

Colorimetry Measurements. UV−vis absorption spectra were recorded on a Cary 300 UV−vis spectrophotometer. A stock solution of surfactant at a concentration about 10 times the expected cac was successively added to 2 mL of deionized water (Purelab Prima Elga, 18.2 MΩ cm) or to 2 mL of 2 mM nucleoside solution, each solution containing 10 μmol.L^{-1} of methyl orange (MO) dye. MO is used as a solvatochromic reporter molecule, as the position of its wavelength absorption band is sensitive to medium effects and surfactant aggregation. In water, the wavelength of maximum absorption of fully hydrated MO is positioned at 463 nm. In the presence of cationic surfactants far below the cac, electrostatic interaction occurs, reflected by a shift of the absorption band to around 380 nm. Upon increasing surfactant concentration, the wavelength of maximum absorption is shifted from 380 nm to about 430 nm, characteristic for MO bound to cationic micelles.[21]

Surface Pressure Measurements. The surface pressure measurements were performed on a computer-controlled Langmuir film balance (Nima Technology, Coventry, UK), and the surface pressure was measured by the Wilhelmy method using a filter paper plate (10 × 23.5 mm^2). Care was taken so that, during the measurements, the bottom edge of the well-soaked plate was always just at the water surface level, still attached to the meniscus.

For the surface pressure isotherms, a rectangular Teflon trough with computer-controlled barriers of 5 × 70 = 350 cm^2 was used. The trough was filled with ultrapure water with the temperature controlled at $T = 21 \pm 2$ °C. The compression rate was 5 cm^2/min, and data points were taken about every 0.05 $Å^2$. Amphiphiles were solubilized in a mixture of chloroform/methanol (9/1) to make solutions on the order of 10^{-4} mol/L. A carefully measured quantity (on the order of 50 μL) of the solutions was spread at the air−water interface with Hamilton syringes. After waiting for 10 min to let the solvents evaporate, the compression curves were registered. The isotherm curves for all the molecules and the mixtures of molecules were repeated at least 3 times and were found to show good reproducibility: the standard deviations of the limiting molecular areas as well as the molecular areas at collapse were less than 5 $Å^2$, and the deviations of the surface pressures at the collapse points were less than 5 mN/m.

Gel/Precipitation Preparation. Nucleoamphiphiles were solubilized in water or nucleosides solution at 40 °C to ensure complete solubilization and then cooled down below T_k in a room with temperature kept at 19 °C to allow gel/precipitation formation.

Optical Microscopy with Differential Interferential Contrast (DIC). Samples sealed between slide glass and cover glass were observed with a NIKON Eclipse PhysioStation E600FN with adequate condensers and prism for DIC observations.

Freeze−Fracture Electron Microscopy. Freeze−fracture experiments were performed with a Balzers vacuum chamber BAF 300 (Balzers, Liechtenstein). A small droplet of mixture was sandwiched between two copper specimen holders. This sandwich was then frozen with liquid propane cooled with liquid nitrogen. The frozen sandwich was additionally fixed to a transport unit under liquid nitrogen and transferred to the fracture replication stage in a chamber that was then pumped down to 10^{-6} mbar at −145 °C. Immediately after the fracture, replication took place by first shadowing with platinum/carbon at an incident angle of 45° and then with carbon deposition at 90°. The sample was allowed to warm to room temperature. Replicas were retrieved and cleaned in water and mounted on 200-mesh copper grids.

Transmission Electron Microscopy. Observations were made with a cryo-electron microscope FEI EM120 (120 kV), and the images were recorded on a Gatan ssCCD camera 2k × 2k. Other samples were fixed by Pt vaporization. The aqueous dispersions of the gels (20 mM) and precipitates (10 mM) were put onto a carbon-coated Cu grid; excess water was blotted with filter paper. For Pt vaporization, we used the same vacuum chamber as for freeze−fracture except that the shadowing was done at 11° and the grid holder was rotated during shadowing.

Scanning Electron Microscopy. Hydrated samples were frozen in liquid propane to avoid water crystallization. After lyophilization, samples were coated with Au/Pd under vacuum and observed using a JEOL GSM 840A microscope operating at 15 kV.

Small-Angle X-ray Scattering. A Rigaku Nanoviewer (Microsource generator, MicroMax 007, 800W rotating anode coupled with a Confocal Maxflux Mirror) was used. Gels and suspensions in water were sealed into a 1.5 mm diameter glass capillary (Glaskapillaren GLAS, Germany). Integrations of the spectra were performed with the program *R-axis Display* software.

(16) In this system, we cannot use buffer solutions, since adding salts such as phosphates will partially replace the counterions which are nucleotides (monophosphate) themselves.

(17) Saito, S.; Moroi, Y.; Matuura, R. *J. Colloid Interface Sci.* **1982**, *88*, 578. (b) Nishikido, N.; Kobayashi, H.; Tanaka, M. *J. Phys. Chem.* **1982**, *86*, 3170.
(18) Sponer, J.; Leszczynski, J.; Hobza, P. *Biopolymers* **2002**, *61*, 3.
(19) Viswanadhan, V. N.; Reddy, M. R.; Bacquet, R. J.; Erion, M. D. *J. Comput. Chem.* **1993**, *14*, 1019.
(20) Davis, J. T. *Angew. Chem., Int. Ed.* **2004**, *43*, 668.
(21) (a) Buwalda, R. T.; Jonker, J. M.; Engberts, J. B. F. N. *Langmuir* **1999**, *15*, 1083. (b) Buwalda, R. T.; Engberts, J. B. F. N. *Langmuir* **2001**, *17*, 1054.

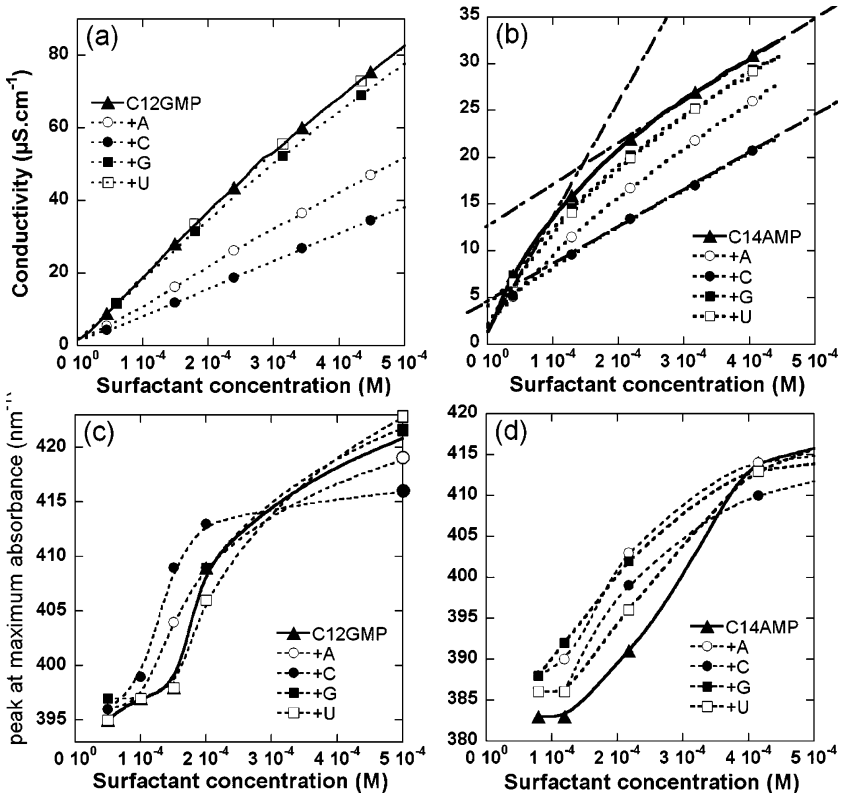

Figure 1. Conductivity and colorimetry measurements of C_{12}GMP and of C_{14}AMP ((a,b) and (c,d) respectively) in pure water and in the presence of 2 mM nucleosides.

Results

Aggregation Behavior around Critical Aggregation Concentration (cac). Surfactant behavior around the cac has been investigated using conductivity and colorimetry measurements, in pure water and in a 2 mM solution of nucleosides (Figure 1). By conductivity measurements (Figure 1a,b), the cac of C_{14}AMP was determined to be around 1.1×10^{-4} M. The break in the conductivity curve of C_{12}GMP was not readily observable. In both cases, addition of some of the nucleosides decreased the conductivity strikingly, but the effect depended on the nature of the nucleoside. U and G only slightly decreased the conductivity, while this effect was more pronounced with A and further enhanced with C, for both nucleoamphiphiles C_{14}AMP and C_{12}GMP.

As the absolute cac values were difficult to precisely determine by this technique, the variation of cac upon nucleoside addition could not be measured for the systems with C_{12}GMP. For C_{14}AMP, the cac decreased along with the absolute conductivity upon addition of C and A.

The effects of added nucleosides on the aggregation behaviors of the nucleoamphiphiles were also investigated by UV−vis spectrometry in the presence of methyl orange (MO) used as reporter molecule (Figure 1c,d). For both C_{12}GMP and C_{14}AMP, the most important change again occurred with the addition of C. Accompanied by a decrease in cac values, dehydration of micelles was observed (lower value of the wavelength at the maximum absorption band above cac: ∼416 nm instead of ∼422 nm for C_{12}GMP and ∼411 nm instead of ∼416 nm for C_{14}AMP). Addition of A and G (only for C_{14}AMP) also decreased the cac values, whereas interestingly, with these nucleosides, the hydration of the micelles was much less affected: the wavelength at the maximum absorption band above cac was similar to that without addition of nucleosides. For both C_{12}GMP and C_{14}AMP, aggregation was only slightly affected upon U addition.

Both the overall conductivity values (0−30 μS.cm^{-1}) and micelle (aggregates) hydration (wavelength at maximum absorption 410−415 nm) measured with C_{14}AMP indicate less ionized and less hydrated micelles than with C_{12}GMP (0−80 μS.cm^{-1} and 415−425 nm, respectively).

The two techniques, conductivity and colorimetry measurements, do not show exactly the same aspect of the phenomenon of aggregation and give complementary information. Conductivity measurements are primarily sensitive to the internucleobase interaction, since the conductivity of the solution reflects the mobility of counterions. At this concentration just above the cac, the pH of the solution is such that all the added nucleosides are uncharged, and the decrease in the conductivity is direct evidence for the association of the added nucleoside to the nucleotide counterions. The observation by colorimetry, on the other hand, is sensitive both to the internucleobase interaction ($\pi-\pi$ stacking and hydrogen bonds) and to the hydrophobicity of the aggregation core where the MO molecules are incorporated. Here, care has to be taken for the interpretation of cac values obtained from the two techniques. Since the MO itself is an amphiphilic molecule with strongly hydrophobic moieties, the inclusion of this molecules, even for a very small quantity (1 for 1000 molecules of nucleoamphiphiles in our case), modifies the cac values.

The purine bases such as GMP and AMP are prone to strong stacking with other purine bases. This leads to the reinforcement of the intermolecular interaction, and an important decrease in cac values is observed with nucleoamphiphiles having purine nucleobases as the counterion in the presence of added purine nucleosides (A and G). On the other hand, such stacking does not seem to influence the hydration of micelles.

The cac values and the hydration of aggregates of C_{12}GMP and C_{14}AMP are also both strongly influenced by the addition of C, whereas they are insensitive to the addition of U. While the effect of C on the C_{12}GMP can be understood in terms of

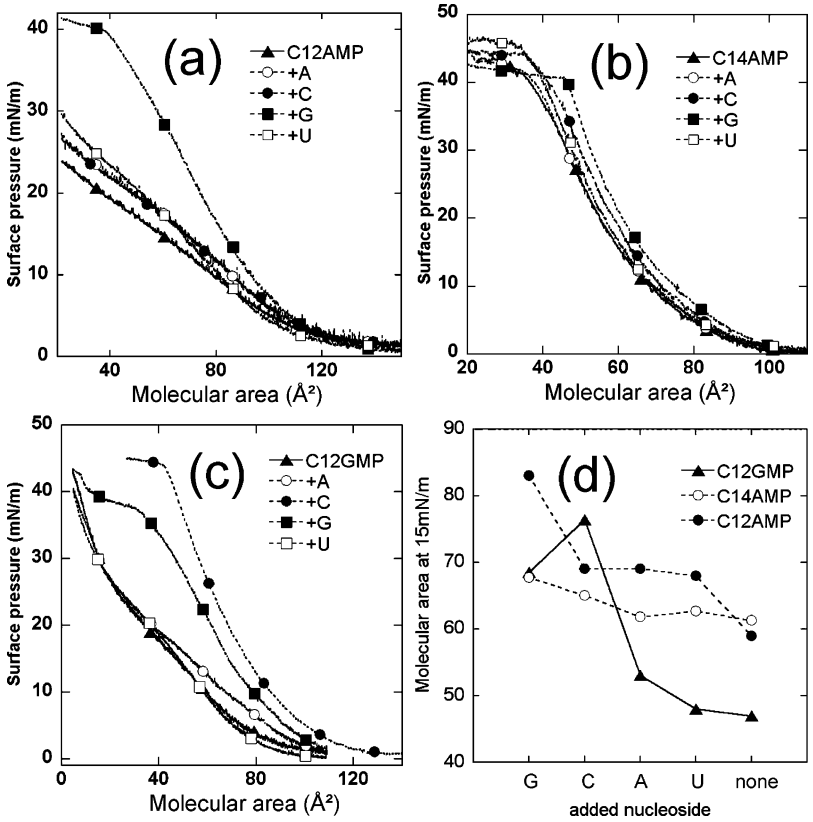

Figure 2. $\pi-A$ isotherm curves of C_{12}AMP (a), C_{14}AMP (b), and C_{12}GMP (c) on pure water and nucleoside subphases. C_{12} amphiphiles alone are too soluble to form stable monolayers, but upon addition of G in the subphase, monolayer formation becomes stabilized. Only with C_{12}GMP does C also have a stabilizing effect. (d) The effect of nucleosides in the subphase on the molecular areas at 15 mN/m.

hydrogen bonds (WC pair),[22,23] the strong effect of C on the C_{14}AMP compared to U is intriguing.[24] Indeed, for the interaction between monomeric nucleobases, Watson−Crick base pairs are far from being the privileged interaction. Contrary to DNA double-stranded helix where isomorphism of base pair is required, in our case, the absence of backbone along with the high mobility of the nucleotides complexed with amphiphiles only with electrostatic interaction allows all possible 28 combinations[4] between two nucleic bases involving at least 2 hydrogen bonds. Furthermore, the hydrophilic character of the nucleoside may play an important role as well. Due to the strong hydrophilicity of uridine, its interaction with the nucleoamphiphiles is not particularly favored compared to a slightly more hydrophobic cytidine whose interaction with an amphiphilic interface is much more favored. It is interesting to note from the cac measurements that, when the interbase interaction is driven by H bonds, it also has an effect on the hydration of aggregates: H bond-driven interaction dehydrates aggregates.

The observation by conductimetry also indicates that the interbase interaction is very important for the conductivity of micellar solutions. For the two amphiphiles, the addition of C decreases most strongly the conductivity of the micellar solution, which can again be understood as a result of H-bonding interaction between the C and the GMP and AMP as observed with colorimetry. The addition of A also decreases the conductivity, which is probably driven by the inter-purine stacking interaction. In this case, again, U does not influence the conductivity, indicating the absence of interactions between the counterion nucleotides and uridine, which is too soluble. What is more intriguing is that the addition of G has almost no effect on the aggregation behavior, whereas it should also exhibit the strong purine−purine interaction with GMP and AMP counterions. A possible reason for this observation may result from the strong hydrophobicity of guanosine. It is extremely difficult to solubilize guanosine even at 2 mM. They simply tend to precipitate. Therefore, in the case of cac measurements, we may not be able to detect all the added G in the vicinity of the micelles of our nucleoamphiphiles.

Surface Pressure Isotherms. Langmuir film compression is a particularly suitable technique to study interactions between surfactants and molecules in solution. It allows controlling the density of deposited functionalized molecules and fixes their orientation.[10,25] Compression of the films on pure water or on nucleoside solution subphases provides insight into how surfactant molecules interact with each other and with nucleosides, since the variation of molecular areas indicates a variation of the packing density, which can be caused by interactions between free nucleobases and the monolayer. Isotherms obtained with C_{12}-AMP, C_{14}AMP, and C_{12}GMP on ultrapure water were compared (Figure 2a,b,c). C_{12}GMP and C_{12}AMP were too soluble to form a stable monolayer alone upon compression, whereas C_{14}AMP exhibits a typical Langmuir isotherm.

Nucleoside Addition. The variation of isotherms upon addition of nucleosides, summarized in Figure 2d as variation of molecular areas at 15 mN/m, showed an interesting tendency: in all cases, the molecular areas increased in the presence of nucleosides in subphase, revealing the presence of interactions between nucleosides and monolayers. However, the amplitude of this interaction

(22) Particularly, the stability of guanine−cytosine (WC) pair is supposedly not very different from the stacked complex.

(23) Florain, J.; Sponer, J.; Warshel, A. *J. Phys. Chem. B* **1999**, *103*, 884.

(24) Acharya, P.; Cheruku, P.; Chatterjee, S.; Acharya, S.; Chattopadhyaya, J. *J. Am. Chem. Soc.* **2004**, *126*, 2862.

(25) Ahlers, M.; Ringsdorf, H.; Rosemeyer, H.; Seela, F. *Colloid Polym. Sci.* **1990**, *268*, 132.

depended strongly on the nature of the nucleobases. The presence of G led to the formation of a stable monolayer for all systems investigated here; because of its strong hydrophobicity, G adsorbs to the air−water interface, inserting themselves in the hydrophobic part of the amphiphiles, stabilizing their monolayers which are otherwise too soluble as is the case for C_{12}GMP and C_{12}AMP. Such behavior has previously been observed with hydrophobic peptide in the subphase.[26] The effect of C in the subphase is very interesting. C has a rather weak effect for C_{12}AMP and C_{14}AMP in terms of expansion of the monolayer. However, it has a strikingly important effect on stabilizing the monolayer of C_{12}-GMP (Figure 2C). As it was observed with G, the presence of C stabilized the monolayer of C_{12}GMP, and a typical isotherm curve was observed under compression, whereas in the absence of C, C_{12}GMP was too soluble to form a stable monolayer. This can be explained neither by the size nor by the hydrophobicity of the nucleoside C. A is a bigger and more hydrophobic nucleoside than C, but has a smaller effect on the monolayer stabilization. Again, the isotherms were only a little (if any) influenced by the presence of U.

It is likely that specific interactions between GMP and C stabilized the presence of the monolayer at interface, which is otherwise too unstable under compression.

Macroscopic Aspect. As indicated by the T_k measurements, at room temperature (∼20 °C), both systems precipitated in water. However, the macroscopic and kinetic aspects of these precipitates were quite different: C_{12}GMP precipitated through two steps. It first formed a clear gel that became opaque with time (Figure 3B). This gel then shrank, forming a white disc (Figure 3C). Water is expelled from the gel in a process of syneresis. This phenomenon induces a decrease in diameter of the disc, becoming denser with time, as shown in Figure 3C. This whole process took about 6 to 8 days. C_{14}AMP on the other hand formed more powder-like precipitates in water: from a solution, it first became opaque (Figure 3E) and then formed a cloudy precipitate (Figure 3F) within hours. For kinetic reasons, as shown in Figure 3, C_{12}GMP had been investigated at 20 mM in water with 2 mM added nucleosides, whereas C_{14}AMP has been investigated at 10 mM in water with 2 mM added nucleosides after having made sure that the morphologies of the assemblies are the same for the two concentrations for both systems.

Nucleoside Addition. Adding nucleosides did not change the macroscopic aspect of the samples, but changed precipitation kinetics. Figure 3a shows the kinetic study of C_{12}GMP aggregation. Addition of C accelerated the syneresis kinetics the most. Syneresis started after 4 days in the presence of C and after 5 and 6 days with A and G, respectively. On the contrary, addition of U tended to slow down syneresis.

Concerning the precipitation of C_{14}AMP, no effects were observed in the presence of G and A, while C tended to slow down the first step of precipitation (from solution to opaque fluid) and U induced a slowing in both steps (Figure 3b).

Microscopy Observations. We have studied the morphology of these aggregates using optical microscopy (OM) and electron microscopy (TEM and SEM). Interestingly, both C_{12}GMP and C_{14}AMP self-assembled to form micrometric fibers and helices, which were clearly visible with optical microscopy. For both cases, the helices were all left-handed. Since the surfactants themselves were not chiral, clearly the chirality of the nucleotide was transcribed and expressed at the supramolecular level.

We followed the different stages of helix formation for the two systems. C_{12}GMP first formed a clear gel with a network

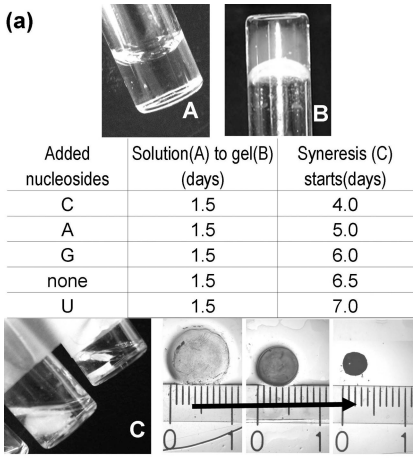

Added nucleosides	Solution(A) to gel(B) (days)	Syneresis (C) starts(days)
C	1.5	4.0
A	1.5	5.0
G	1.5	6.0
none	1.5	6.5
U	1.5	7.0

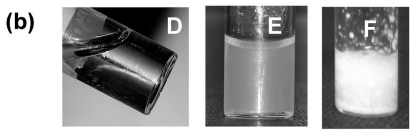

Added nucleosides	Clear (D) to Opaque (E) solution (hours)	precipitates (F) (hours)
G	1.5	3.0
A	1.5	3.0
none	1.5	3.0
C	2.5	3.0
U	3.0	6.0

Figure 3. Kinetics of precipitation of C_{12}GMP (a) and C_{14}AMP (b): showing the different steps of precipitation as a function of added nucleoside. A−C for C_{12}GMP, where solutions gel first, then undergo syneresis, and the diameter of the gels decreases with time (the interval time between gels shrinking from 9 mm to 6 mm and 3 mm is 7 to 10 days). The gels appear black on the images with a ruler, since this is done with a transmission binocular microscope; as the gels become denser through syneresis, they appear black with the transmission method. D−F for C_{14}AMP, clear solutions form cloudy precipitates.

of nanometric tubule-like structures with a diameter of 10 nm observed by TEM (Figure 4A). These fibers self-assembled with time, forming a network observable under OM along with the formation of helical structures (Figure 4B). The gels became opaque at the same time.

C_{14}AMP precipitated, forming very fine nanometric needles first (Figure 5A). TEM and SEM images obtained at this stage showed chiral multilayered cigar-like rolled structures at the nanometric level. Long and thicker fibers then appeared, and micrometric helices started to form in parallel (Figure 5B). Helix density increased with time along with fiber density. The two structures continued to coexist.

Nucleoside Addition. With G and U, the morphologies of the assemblies of C_{12}GMP did not show particular variation, whereas in the presence of A and C, accelerated and enhanced nucleation leading to whiter gels were observed (Figure 6). This is in agreement with the kinetic behavior as observed in the Figure 3.

Concerning the morphologies of the aggregates observed with C_{14}AMP, the addition of U, G, and A did not have any particular effect (with a hint of the presence of larger helices with U), whereas the addition of C completely suppressed helix formation. Only long fibers were observed (Figure 7). Again, this indicated that the variation of aggregate formation kinetics as it was observed in the Figure 3 did influence their morphologies, as only C and U have affected the kinetics.

If we summarize the macroscopic and mesoscopic behaviors, the self-assembly of the amphiphilic molecules is extremely sensitive to the molecular structure and additives. C_{12}GMP forms

(26) Caetanoa, W.; Ferreirab, M.; Oliveira, Jr., O. N.; Itri, R. *Colloids Surf., B: Biointerfaces* **2004**, *38*, 21.

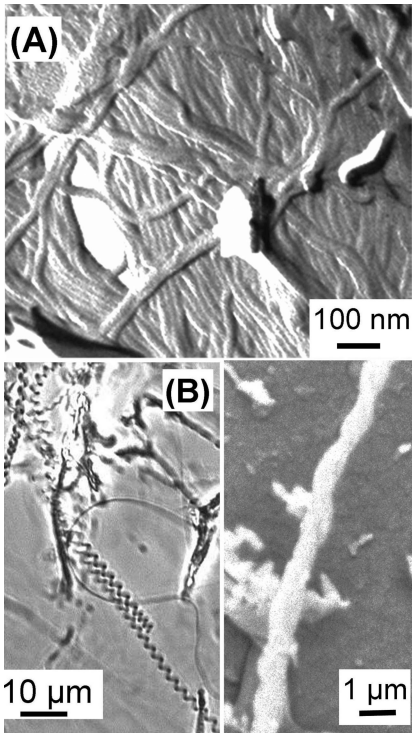

Figure 4. OM, TEM, and SEM images of helix formation in pure water resulting from the self-assembly of C_{12}GMP. While it is still in its solution state (A), nanometric fibers without apparent chiral shape start to appear after 1 day. As it starts to gel (B), microscopic helices probably formed by intertwining of the nanometric fibers appear (images taken after 3 days).

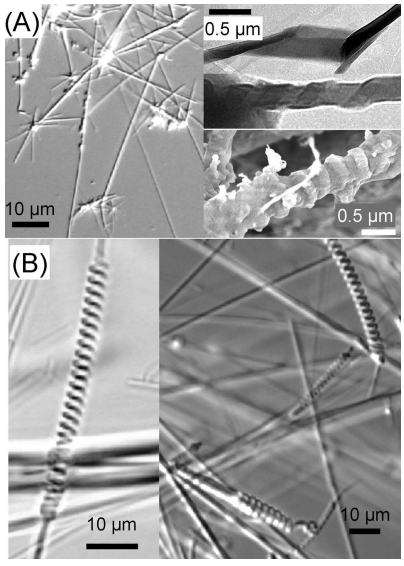

Figure 5. OM, TEM, and SEM images of left-handed helix formation in pure water resulting from the self-assembly of C_{14}AMP. At the early stage of aggregation (after 1 h) (A), only very fine needles with diameter of a few hundred nanometers were observed. The detailed observation by TEM showed rolled multilayer cigar-like tubes with left-handed chirality forming these needles. After 3−4 h (B), some of these needles transformed to micrometric helices.

3D networks of micrometric fibers which then form gels that undergo syneresis within days, while C_{14}AMP forms a cloudy precipitate within hours. The mesoscopic structures of these aggregates observed using OM, TEM, and SEM have shown that the self-assemblies of these nucleoamphiphiles express chirality at the supramolecular level, and the helices are formed in a hierarchical manner, first at nanometric scales (tubular

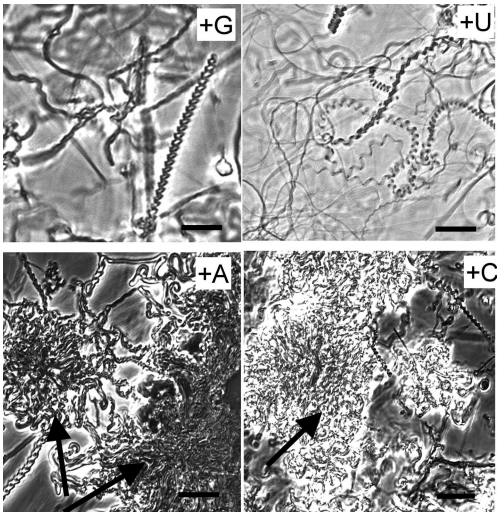

Figure 6. Optical microscopy images of micrometric helices obtained with C_{12}GMP (20 mM) in the presence of nucleosides in water (2 mM). In the presence of G and U, the aspects of gels remain the same to those without nucleoside. With A and C, accelerated gel formation with highly entangled domains (arrows) is observed. Scale bar 10 μm.

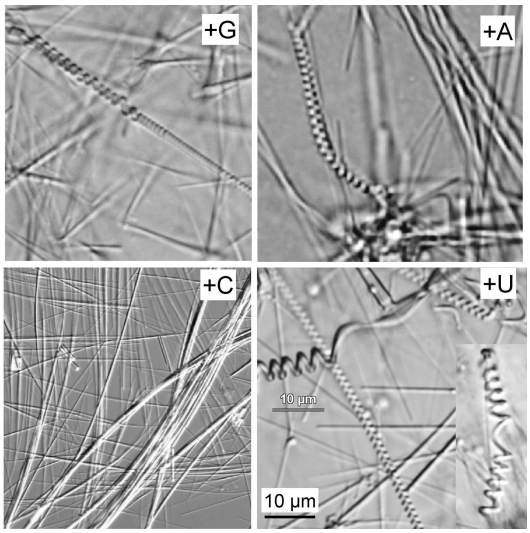

Figure 7. Optical microscopy images of micrometric helices obtained with C_{14}AMP (10 mM) in the presence of nucleosides in water (2 mM). In the presence of G, A, and U, the aspects of helices are not greatly influenced (with some larger helices with U). In the presence of C, no helices are observed.

structures for C_{12}GMP and cigar-like rolled fiber structure for C_{14}AMP); then, such structures assemble into optically visible chiral helical structures at micrometric scales. Since the only chiral centers are found in the sugar groups of nucleotides, the supramolecular chirality expression is induced by the counterions, as several other examples that we have previously reported with tartrates and peptides. Adding nucleosides changes both the kinetics of precipitation and the morphologies of the aggregates. Again, aggregation in the presence of C and, to lesser extent of A presents the most dramatic changes to both systems; in the presence of C, C_{14}AMP does not form micrometric helices, and only micrometric needles are observed, whereas the kinetics of gel formation of C_{12}GMP and the syneresis are both accelerated by the presence of C and A, and locally strongly entangled nucleation points are observed.

Intermolecular Interactions (NMR Study). We have studied intermolecular interactions between nucleoamphiphiles and

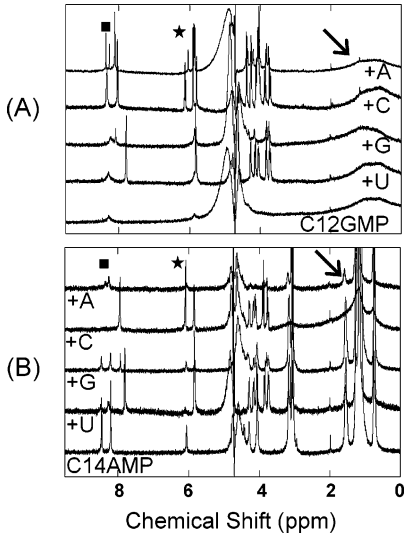

Figure 8. 400 MHz ^{1}H NMR full spectra of C_{12}GMP (A) and C_{14}AMP (B) alone and with added nucleosides in D_2O. Arrows show surfactant moieties, (■) show nucleobase, and (★) show sugar moieties (H1′).

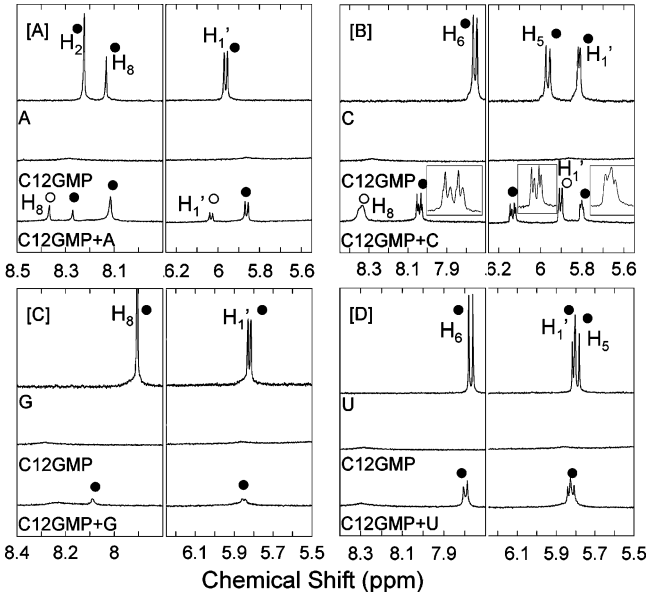

Figure 9. ^{1}H NMR spectra of C_{12}GMP (20 mM) with added nucleosides (2 mM) in D_2O. Two regions of the spectra are shown with base protons (7.6−8.6 ppm) and in the 1′ proton of the sugar moieties (5.7−6.2 ppm). In each case, we compare the spectra of the nucleoside alone, of C_{12}GMP alone, and in the presence of the nucleoside.

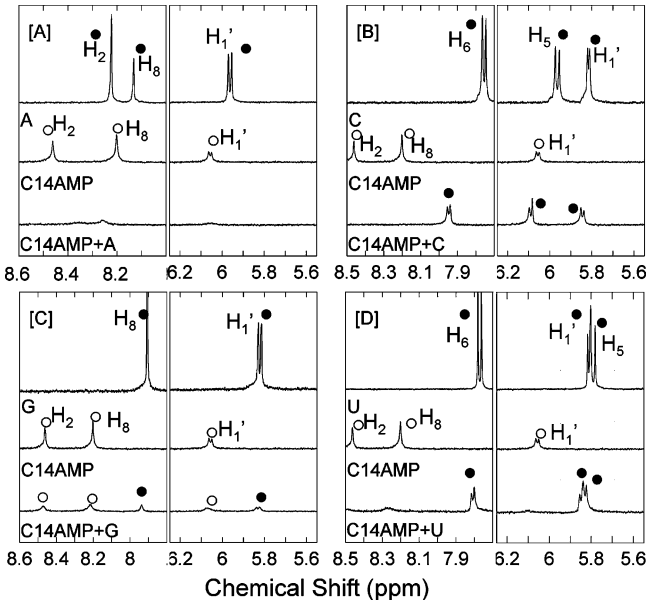

Figure 10. Intermolecular interaction study of C_{14}AMP (10 mM) with added nucleosides (2 mM) by 400 MHz ^{1}H NMR in D_2O. Parts of 400 MHz ^{1}H NMR spectra in the region of the base protons (7.6−8.6 ppm) and in the 1′ proton of the sugar moieties (5.7−6.2 ppm). In each case, we compare the spectra of the nucleoside alone, of C_{14}AMP alone, and in the presence of the nucleoside.

nucleosides in solution using 400 MHz ^{1}H NMR. The amphiphilic molecules in their solid-like aggregated form (precipitate or gel) should not show peaks with fine resolution; on the other hand, the counterions have a more or less stronger interaction with the head groups of the surfactants, and we could probe this interaction as well as the interaction between counterions (nucleotides) and the added nucleosides in solution. The first striking observation concerns the full spectra of both surfactants without addition of nucleosides (the bottom spectra of Figure 8 A,B). In C_{12}GMP systems, protons corresponding to the hydrophobic chains of amphiphiles (arrow, Figure 8A) are not resolved, as well as those of the ribose and H8 of GMP (black star and black square, respectively; Figure 8A), typical signature of the solid-like aggregated state. However, surprisingly, both amphiphilic moieties of C_{14}AMP (arrow, Figure 8B) and nucleotides AMP (black star and black square, respectively; Figure 8B) exhibit fine resolution in ^{1}H NMR. Since the Krafft temperature and the cac of both amphiphiles are comparable, C_{14}AMP should not be more soluble with higher monomeric concentration in the solution state with finely resolved ^{1}H NMR peaks.

Although they both form macroscopic helices, the dynamical properties of the organization of the two surfactants inside the helices at molecular level are clearly different, and the hydrophobic chains of precipitate forming C_{14}AMP show, although they are less soluble, more dynamical behavior.

We have then investigated intermolecular interactions between the surfactant and each nucleoside by particularly focusing on the protons of the base (7.6−8.6 ppm, black square) and on the H1′ of the sugar moieties (5.7−6.2 ppm, black star). We compared the three spectra of the (1) nucleoside alone and of the surfactant (2) alone and (3) in the presence of four different nucleosides for both C_{12}GMP and C_{14}AMP in Figure 9 and 10, respectively.

C_{12}GMP in the Presence of Nucleosides. In C_{12}GMP systems, adding A or C induces similar behaviors on a first approach. In each region of interest, we observed that new peaks appeared (open circles in Figure 9) upon nucleoside addition at around 8.35 and 6.05 ppm in (A) and 8.35 and 5.9 ppm in (B). These signals can be attributed, respectively, to H8 and H1′ of the C_{12}GMP. No significant chemical shift of the adenosine was observed when mixed with C_{12}GMP, except that the H1′ signal of adenosine is shifted upfield by 0.1 ppm. Upon cytidine addition, the chemical shift of this peak was unchanged, whereas H5 and H6 of the base are shifted downfield by 0.15 and 0.2 ppm, respectively. Finally, all cytidine signals are doubled with a 2:1 ratio corresponding to two different species on the NMR time scale. These two sets of peaks can reasonably be assigned to the free cytidine and the cytidine interacting with C_{12}GMP. This is confirmed by the surprising appearance of GMP signals, which can correspond to weakened GMP−surfactant interactions in the presence of C. Nevertheless, both cytidine signals (free and interacting) are affected by the gel environment.

In the presence of G and U, the observed peaks corresponded to the sum of the two spectra (GMP + G or GMP + U). However,

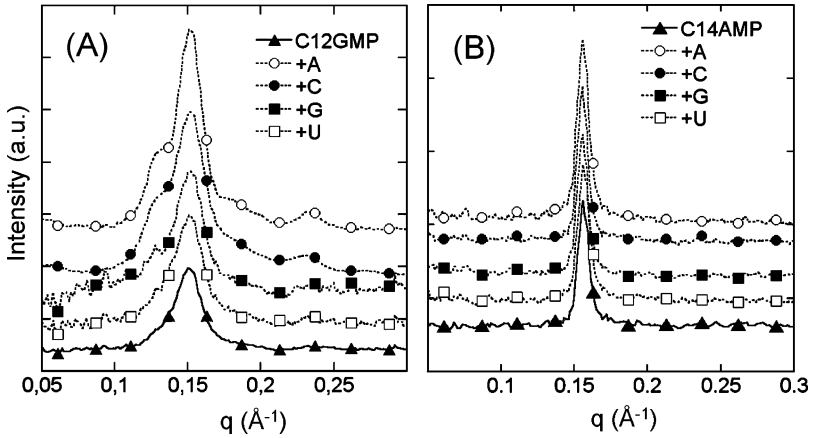

Figure 11. X-ray scattering patterns of C_{12}GMP (A) and of C_{14}AMP (B) in the presence of nucleosides in the SAXS regime. While adding nucleosides to C_{12}GMP samples induces some variation in SAXS patterns, no effects are observed with C_{14}AMP.

the behaviors were different. The uridine signals were slightly broadened but did not exhibit chemical shift variation as was expected for the free nucleoside in solution. The interactions between nucleosides, if any, were not strong enough to influence the environment of nucleotides. A 0.3 ppm downfield shift was observed for guanosine H8, and both H8 and H1′ signals were broadened, with low signal/noise ratio indicating that guanosine does interact with GMP; but either only very little guanosine remains in solution (they are simply not soluble and precipitate separately), or a strong insertion of guanosine in the surfactant aggregates makes them immobilized at the aggregate surface.

C_{14}AMP in the Presence of Nucleosides. Regardless of added nucleoside, the AMP signals (open circles in Figure 10) were broadened, and their intensities were significantly decreased (G, U) or disappeared completely (A, C) as is observed in Figure 10. In the case of added adenosine (A), very little signal was observed: all the molecules seemed to be involved in the precipitation with stronger interaction (C_{14}AMP and AMP-A) of the system. For cytidine (B), at least a part remained free in solution as shown by the well-resolved nucleoside (cytidine) signals. A 0.2 ppm downfield shift was observed for H6. The addition of guanosine, as in the previous case, showed relatively little effect on nucleotide signals and the nucleoside signal disappeared almost completely. Uridine addition exhibited a slight broadening of its signals corresponding to the free species in solution.

To summarize the NMR data, only extremely weak interactions between uridine and GMP and AMP surfactants are observed; the nucleoside remains free in solution. The opposite behavior is observed with guanosine: low soluble proportion and with relatively weak interaction with the nucleotide. However, both A and C interact with the counterions (AMP and GMP) of both surfactants. Different behaviors are observed, depending on the nature of the nucleotide. The signals due to AMP are observable with C_{14}AMP, although they are precipitated, which indicates some mobility of the counterions even in the middle of the precipitates. Upon addition of nucleosides, in particular, C and A, these signals disappear; the nucleosides tend to immobilize AMP. On the other hand, in the case of GMP, interactions of the nucleosides C and A tend to "solubilize" the nucleotides, causing the appearance of the corresponding signals. In both cases, adenosine is completely involved in the process instead of cytidine, which is partially free in solution.

The pH of the C_{12}GMP solutions in the concentration (20 mM) studied here (see Supporting Information) is below the pK_a values of cytosine and adenine in solution (4.17 and 3.52, respectively). A priori both cytidine and adenosine are positively charged (protonation at N3 and N1, respectively), which should prohibit their interaction with the positively charged amphiphilic assemblies. The influence of C and A nucleosides, which are observed both for C_{12}GMP and for C_{14}AMP, may result from their inherent propensity to adsorb at the amphiphilic interface. Moreover, the pK_a values of nucleosides may be different at the amphiphilic interface environment from that in the bulk solution, and they may remain uncharged. Regardless on the protonation state, C and A nucleosides are those that have the strongest influence on the assembling behaviors.

Small-Angle X-ray Scattering (SAXS). The precipitates were also studied with SAXS. Scattering patterns of C_{14}AMP and C_{12}GMP both exhibited Bragg-type peaks at around $q = 0.15$ Å^{-1} (Figure 11), which corresponded to periodicity of about 42 Å. These peaks were attributed to a well-organized periodic stacking of bilayer structures with very little water embedded between, as was revealed by the TEM image in the case of C_{14}-AMP with the multilayered cigar-like structures. In the case of C_{12}GMP (Figure 11A), the peaks were a little broader. This probably reflected the smaller number of bilayer stacking in the primary tubule-like structures.

Nucleoside Addition. With the addition of A and C to C_{12}-GMP, a shoulder peak appears at around 0.125 Å^{-1} along with the principal peak at 0.15 Å^{-1} (Figure 11A), whereas U and G do not have any effect on the scattering pattern. In the case of C_{14}AMP, adding nucleosides does not induce any change in the scattering spectra. (Figure 11B). It is interesting to note that the important morphological changes of the aggregates with the addition of nucleosides (e.g. C_{14}AMP + C) are not reflected in the assembly at scales investigated by SAXS.

We have combined different techniques such as conductimetry, colorimetry, Langmuir monolayer, microscopy, ^{1}H NMR, and small-angle X-ray scattering to investigate the assembling behavior of new nucleoamphiphile systems C_{12}GMP and C_{14}-AMP as well as their interactions with nucleosides at different levels: molecular and supramolecular as well as nanometric and micrometric scales. All these results unanimously indicate that, regardless of the nature of the counterions−nucleotides, the nucleosides which interact most with the amphiphilic aggregates are cytidine and adenosine. As we have previously mentioned, due to the competition with the hydrogen bonds in water molecules, the interactions among mononucleotides are not favored in solution. However, the surfaces of the amphiphilic aggregates can confine these nucleotides and induce intermolecular interaction. The mechanisms which govern such interactions are quite complex, as the Watson−Crick base pairs are far from being the privileged pairs between monomeric nucleobases.

Table 1. Schematic Summary of Microscopical Aspects of Helices as a Function of Added Nucleosides

	Alone	+C	+A	+G	+U
C12GMP					
C14AMP	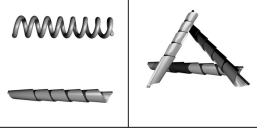				

Practically all bases do interact with all the others. The reason we have observed different effects depending on the nucleosides probably lies elsewhere. The different nucleosides have different solubilities, in the order G < A < C < U. As these nucleosides in solution are in contact with amphiphilic aggregates, what we observe is a cooperative effect between the hydrophobicity/hydrophilicity of nucleosides, which will predispose them at the amphiphilic interface. This works then cooperatively with their possibility of forming hydrogen bonds and/or stacks with the counterions confined at the interface. In comparison to guanosine, which is not very soluble, thus does not remain in solution, and to uridine, which is very soluble and does not have particular affinity to the amphiphilic interface, cytidine and adenosine seem to have the "right range" of the propensity to adsorb at the interface, as reflected by their stronger influence on the self-assembling behaviors. Particularly, cytidine has a stronger capacity to form hydrogen bonds based on one of the many possibilities both with C_{12}GMP and with C_{14}AMP.

Conclusion

We described new self-assembling systems based on nucleoamphiphiles. Nano to micrometric left-handed helix formation with stacked bilayer-type aggregates was induced simply by complexing chiral GMP or AMP with a nonchiral monocationic amphiphile without any covalent connection between both elements. This provides a new example of supramolecular chirality expression through molecular chirality transfer from counterions to amphiphiles.

Studying the nucleoamphiphiles in aqueous solution in the presence of nucleosides (adenosine, guanosine, cytidine, and uridine) allows getting insights into the weak interactions between nucleobases and amphiphilic assemblies. The presence of nucleosides in the solution influences the kinetics and morphology of aggregation and monolayer formation at the air−water interface of C_{14}AMP and C_{12}GMP in a subtle manner. This is induced by cooperative effects amonf π stacking, hydrophobicity of the bases, and hydrogen bonding. Interestingly, regardless of the nucleoamphiphiles, cytidine most strongly influenced the kinetics and morphologies of aggregate formation, showing the strongest association with the amphiphilic aggregates by decreasing the conductivity of the solution or by stabilization of the monolayer at the water surface. Adenosine also has influence on these phenomena. The detailed observation around the cac revealed the complexation of C to GMP or AMP, resulting in dehydration of micelles. Therefore, the interaction is likely driven by hydrogen bonding, whereas the complexation of A with the AMP and GMP does not influence the hydration of the aggregates: the interaction is likely driven by $\pi-\pi$ stacking or hydrophobic effect between purine bases. Uridine has very little effect on the assembling behavior of the nucleoamphiphiles, probably because of its hydrophilicity and its weakest capacity for interaction. Interestingly, G, which should interact also with purine-based counterions, has less effect on the organization of AMP or GMP. It is likely that, due to its strong hydrophobicity, G precipitates separately and/or interacts preferentially with the hydrophobic core of the aggregates rather than with nucleotide counterions. The proton environment of nucleobases as well as the sugar moieties of the nucleotides as detected with NMR also confirmed that GMP and AMP were most perturbed in the presence of C and A. The ensemble of these observations indicates that, with the system reported here, where the nucleotides and the amphiphiles are complexed with electrostatic interaction to form the nucleoamphiphiles, the interaction between the nucleosides in solution and the nucleoamphiphilic aggregates occurs in a cooperative manner. The primary driving force is the hydrophilic/phobic character of the nucleoside. Extreme properties, i.e., like very hydrophilic U and very hydrophobic G, do not induce specific interactions with the nucleoamphiphiles. Intermediate properties allow vicinal interactions between nucleoside and complexed nucleotides. In such cases, hydrogen bonding and $\pi-\pi$ stacking interactions can take place, without any restriction to Watson−Crick pairing. The important decrease of the conductivity of the micellar solution along with the NMR measurements clearly demonstrates that, within the right range of hydrophobicity, the nucleosides at the aggregate interface do interact with nucleotide counterions through weak interactions. This is probably why the nucleosides cytidine and adenosine with their intermediate solubility have the strongest effects on the several assembling properties of the nucleoamphiphiles investigated here. Roughly, the effect of the nucleosides can be classed in the order C > A > G ≥ U regardless of the complexed nucleotides. Such observations are further in agreement qualitatively with our previous report[13] where we studied the aggregation behavior of UMP−cationic gemini surfactant complex, and the observed effect of the added nucleoside on the assembling behavior of the nucleo-gemini followed the order C ≥ A > G ≥ U. The fact that adenosine strongly interacts with UMP counterion whereas uridine does not interact with AMP counterions also confirms that it is primarily the hydrophobicity of the nucleoside and not the pair properties of nucleotides−nucleosides that governs the interaction capacity of the nucleosides and nucleoamphiphiles aggregates.

In this study, we took advantage of the ability of nucleic acids to interact via a diversity of weak bonds along with the intrinsic aggregation properties of amphiphiles. We have shown that the added nucleosides play important roles as a result of complex combination of weak interactions. Understanding the mechanism of interaction between these bioinspired building blocks is extremely important to control self-assembly and to design new bioarchitectures.

Acknowledgment. The authors are grateful to A. Grelard for her help on NMR measurements. K.Y.P. thanks Emory University for the fellowship which allowed her to work at IECB for 2 months. T.S. acknowledges Japanese Government for the "Collège Doctoral Franco-Japonais" program.

Supporting Information Available: Additional experimental information as described in the text. This material is available free of charge via the Internet at http://pubs.acs.org.

LA702105S